

Perturbation Theory Eigenvalue Sensitivity Analysis with Monte Carlo Techniques

B. T. Rearden*

Oak Ridge National Laboratory
P.O. Box 2008, Oak Ridge, Tennessee 37831-6370

Received January 9, 2003

Accepted June 30, 2003

Abstract—Methodologies to calculate adjoint-based first-order-linear perturbation theory sensitivity coefficients with multigroup Monte Carlo methods are developed, implemented, and tested in this paper. These techniques can quickly produce sensitivity coefficients for all nuclides and reaction types for each region of a system model. Monte Carlo techniques have been developed to calculate the neutron flux moments and/or angular fluxes necessary for the generation of the scattering terms of the sensitivity coefficients.

The Tools for Sensitivity and Uncertainty Analysis Methodology Implementation in three dimensions (TSUNAMI-3D) control module has been written for the Standardized Computer Analyses for Licensing Evaluation (SCALE) code system implementing this methodology. TSUNAMI-3D performs automated multigroup cross-section processing and then generates the forward and adjoint neutron fluxes with an enhanced version of the KENO V.a Monte Carlo code that implements the flux moment and angular flux calculational techniques. Sensitivity coefficients are generated with the newly developed Sensitivity Analysis Module for SCALE (SAMS). Results generated with TSUNAMI-3D compare favorably with results generated with direct perturbation techniques.

I. INTRODUCTION

The usefulness of sensitivity analysis techniques for reactor safety applications has been demonstrated repeatedly over the last 30 yr. Application of sensitivity theory has included assessing the impact of small deviations in reactor parameters, as well as determining the effect of nuclear data on the multiplication factor.^{1,2} Recently, multigroup sensitivity and uncertainty (S/U) techniques have been used to determine the area of applicability (AOA) of critical experiments.^{3,4} This work requires groupwise sensitivity coefficients for multiple reaction types for every nuclide in each system included in the analysis. Two sensitivity analysis sequences have been developed for the Standardized Computer Analyses for Licensing Evaluation (SCALE) code system.⁵ The SEN1, a one-dimensional (1-D) sensitivity analysis tool based on deterministic neutron transport,⁶ was developed to test these new AOA techniques. Once favorable results were demonstrated, the

SEN2 prototypic two-dimensional (2-D) sensitivity analysis tool,⁶ also based on deterministic neutron transport, was developed. Initial application of these codes³ to criticality safety analyses demonstrated the potential benefit that would be provided by implementing the S/U techniques into a three-dimensional (3-D) Monte Carlo code, which is the computational approach often needed to model the geometric complexity important for accurate prediction of the effective neutron multiplication factor (k_{eff}) for a system. The differential operator perturbation options available in recent releases of the MCNP code⁷ could lend themselves to this type of analysis, but the computational time would likely be prohibitive. This is because the AOA techniques require a comparison of the sensitivity coefficients for each of the systems under consideration on an energy-dependent basis for multiple nuclear reaction types for each nuclide in each system. Because of the large number of energy-dependent sensitivity coefficients required by the AOA techniques, the adjoint-based first-order-linear perturbation theory approach to sensitivity analysis was chosen as the solution methodology.

*E-mail: reardenb@ornl.gov

Several sensitivity analysis codes have been written that apply first-order-linear perturbation theory to forward- and adjoint-flux solutions obtained with deterministic neutron transport techniques. However, prior to this work, this approach to sensitivity analysis had never been applied to a production-level Monte Carlo code. The calculation of the sensitivity coefficients, as implemented in this methodology, requires the determination of the forward and adjoint energy-dependent scalar neutron fluxes as well as the moments of these fluxes. Previously, no methodology existed for the generation of the moments of the neutron flux with Monte Carlo techniques. The flux moments are necessary for the computation of the group-to-group transfer components of the sensitivity coefficients. In Sec. II of this paper, two new techniques for the generation of flux moments with Monte Carlo techniques are presented. Section II also presents the techniques for the generation of sensitivity coefficients. Section III presents the implementation of this methodology into the SCALE code system. Section IV contains verification cases and sample calculations. These descriptions demonstrate the consistency of results generated with the SCALE sensitivity analysis sequence and those generated through direct perturbation techniques. Finally, Sec. V presents conclusions drawn from this work and recommends further enhancements to improve upon this work.

II. METHODS

The application of first-order-linear perturbation theory to Monte Carlo techniques is presented in this section. The most complex component of this implementation is the calculation of the group-to-group transfer terms. Because the transfer (or scattering) cross sections are stored in a Legendre expansion, the neutron fluxes must be calculated in terms of the flux moments. In three dimensions, this requires a spherical harmonics expansion of the neutron flux. Geometrical configurations typically used in Monte Carlo analyses are not well suited for the classical approach to the calculation of neutron flux moments as is commonly used in deterministic neutron transport codes. Monte Carlo models for criticality safety often involve large geometric regions and multiple use of the same region in arrays.

A new approach to compute flux moments using coordinate transformations to calculate the spherical harmonics components of the flux solution using Monte Carlo methods is presented in Sec. II.A. The use of a coordinate transformation to calculate an angular flux solution with Monte Carlo methods, and then compute the flux moments through a spherical harmonics expansion, is presented in Sec. II.B. Reviews of techniques applied later in this paper to generate sensitivity coefficients from the flux moments and the cross-section data are presented in Secs. II.C and II.D.

II.A. Calculation of Flux Moments with Monte Carlo Techniques

Deterministic neutron transport codes calculate the moments of the forward and adjoint fluxes for each region on a fixed spatial and energy mesh through a series expansion using spherical harmonics. With some modifications, this methodology can be applied to the calculation of flux moments with Monte Carlo methods. Based on an angular flux solution obtained over a discrete angular quadrature, the j 'th real valued flux moment for energy group g and region z can be calculated as follows⁸:

$$\tilde{\sigma}_{g,z}^j = \sum_{n=1}^N w_n R_n^j \phi_{g,z}^n, \quad (1)$$

where

$\phi_{g,z}^n$ = neutron flux in region z , for direction n and energy group g

w_n = weight function for direction n

R_n^j = real-valued spherical harmonics function for moment index j and quadrature direction n

N = number of directions in the angular quadrature set.

Using the track length estimator method in a Monte Carlo calculation, the groupwise scalar flux within a single region for a single generation of particles is calculated as^{9,10}

$$\phi_{g,z} = \frac{\sum_{k=1}^K W_{k,z} l_{k,z}}{V_z \sum_{k=1}^K W_{k,0}}, \quad (2)$$

where

$l_{k,z}$ = distance traversed by particle k while within region z and energy group g

$W_{k,z}$ = weight of particle k while traversing region z

V_z = volume of region z

$W_{k,0}$ = initial weight of particle k

K = total number of histories in the generation.

New techniques have been developed to calculate flux moments via Monte Carlo methods. The flux moments are tallied in a method similar to that used to calculate the scalar flux, with only one additional term. Through this technique, each tally is treated in a similar manner to each solution direction in discrete ordinates techniques. Each flux moment is calculated as

$$\tilde{\phi}_{g,z}^j = \frac{\sum_{k=1}^K R_k^j W_{k,z} l_{k,z}}{V_z \sum_{k=1}^K W_{k,0}}, \quad (3)$$

where R_k^j is the real-valued spherical harmonics function for moment index j corresponding to the direction of particle k .

In Eq. (3) the real-valued spherical harmonics functions are calculated for each history using a transformed coordinate system such that the moments are based on a polar rather than Cartesian position vector. This is a 3-D extension of the 1-D method for calculating the flux moments in terms of Legendre polynomials based only on μ , the direction cosine with respect to the spatial coordinate.

This coordinate transform is illustrated in Fig. 1. Here, $\hat{i}, \hat{j},$ and \hat{k} represent the directional coordinate system axes; $\mu, \eta,$ and ξ represent the direction cosines; and θ and ρ represent the polar and azimuthal angles of the “normal” coordinate system. The same symbols “primed” represent the transformed coordinate system. Here, the transformed polar or \hat{k}' axis is colinear with the position vector \vec{r}_c directed from the center of the region for which moments are desired to the point at

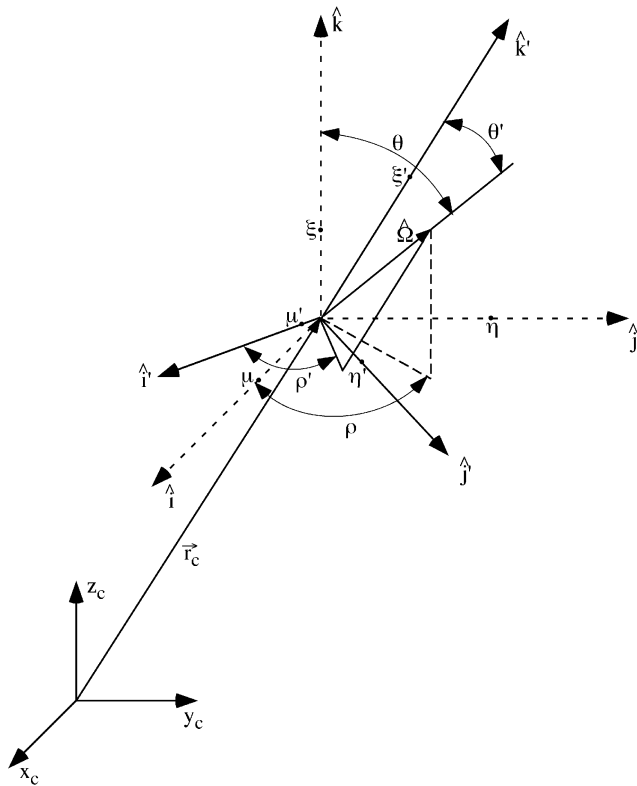


Fig. 1. Coordinate system transform for spherical harmonics expansion.

which the flux tally occurs. By using the center of the region as a reference point, consistency of the moment calculation is assured with differing models of the same system. The \hat{i}' and \hat{j}' axes are chosen to form an orthogonal coordinate system with \hat{i}' held in the plane formed by \hat{i} and \hat{j} . The use of constraints other than the restriction of \hat{i}' to this plane may be explored in future studies. If an additional constraint is not placed on either \hat{i}' or \hat{j}' , the transform would be able to rotate about \hat{k}' , and the consistency of consecutive transformations of the same direction could not be assured. With the transform computed, the position and direction of travel of the particle remain unchanged, but the spherical harmonics terms are calculated using the transformed coordinate system. With the direction cosines consistently transformed for each history, the new polar and azimuthal angles can be computed, and the spherical harmonics functions can be calculated for each history. The flux moments can then be tallied as shown in Eq. (3).

Although this methodology produces accurate solutions, the computational cost is high. Each time a particle’s contribution to the flux is tallied, the angular transformations and the spherical harmonics components must be calculated.

II.B. Calculation of Angular Fluxes with Monte Carlo Techniques

In order to improve the efficiency of the calculation, an alternative technique was devised such that the angular flux is tallied within the Monte Carlo code. These angular fluxes are stored, and after the Monte Carlo calculation is complete, a spherical harmonics expansion of this solution is performed to obtain the flux moments. The method for the calculation of the scalar flux as presented in Eq. (2) is easily modified to calculate the group-wise angular flux in a region as

$$\phi_{g,z}^n = \frac{\sum_{k=1}^K W_{k,z} l_{k,z,n}}{V_z \sum_{k=1}^K W_{k,0}}, \quad (4)$$

where $l_{k,z,n}$ is the distance traversed by particle k while within region z and energy group g within the quadrature direction n .

In Eq. (4) the direction of travel for each history is calculated in reference to the same transformed coordinate system as presented in the previous section and shown in Fig. 1. The use of this technique for the calculation of the flux moments provides a significant improvement in the computational efficiency over the previously described method of calculating the flux moments directly in the Monte Carlo code. Although the coordinate transform must still be performed for each flux tally, the spherical harmonics components no longer have to be repetitively calculated. Instead, the direction

of travel must be checked for storage in the proper quadrature direction. Any of a wide variety of angular quadrature sets could be used to produce the angular fluxes using this methodology. An example application of this methodology is presented in Sec. III.A.

II.C. Explicit Sensitivity Coefficient Generation

Using the foregoing methodologies to calculate the flux moments for the forward and adjoint solutions, the flux information necessary to compute the sensitivities of k_{eff} to the cross-section data using multigroup Monte Carlo methods is available. The same problem-dependent cross-section set used to generate the Monte Carlo solution is also used for the generation of the sensitivity coefficients. A review of methods used to generate the sensitivity coefficients is presented in this section. This methodology is identical to that used in the FORSS code system¹¹ for fast reactor applications, with the addition of the sensitivity of k_{eff} to the fission energy spectrum⁶ (χ). The sensitivity coefficients produced with these techniques give the sensitivity of the computed k_{eff} to a particular groupwise cross-section data component, the so-called explicit sensitivity coefficients.¹²

In operator notation, the eigenvalue-neutron-transport equation can be expressed as

$$A\phi = \frac{1}{k} B\phi, \quad (5)$$

where

ϕ = neutron flux

$k = k_{eff}$, the largest of the eigenvalues

A = operator that represents all of the transport equation except for the fission term

B = operator that represents the fission term of the transport equation.

The adjoint form of the transport equation can be expressed as

$$A^\dagger \phi^\dagger = \frac{1}{k} B^\dagger \phi^\dagger. \quad (6)$$

In the adjoint equation, the adjoint flux ϕ^\dagger has a special physical significance as the ‘‘importance’’ of the particles within the system.

Using linear perturbation theory, one may show that the relative change in k due to a small perturbation in a macroscopic cross section Σ of the transport operator at some point in phase-space \vec{r} can be expressed as

$$S_{k,\Sigma(\vec{r})} \equiv \frac{\Sigma(\vec{r})}{k} \frac{\partial k}{\partial \Sigma(\vec{r})} = - \frac{\Sigma(\vec{r})}{k} \frac{\left\langle \phi^\dagger(\vec{\xi}) \left(\frac{\partial A[\Sigma(\vec{\xi})]}{\partial \Sigma(\vec{r})} - \frac{1}{k} \frac{\partial B[\Sigma(\vec{\xi})]}{\partial \Sigma(\vec{r})} \right) \phi(\vec{\xi}) \right\rangle}{\left\langle \phi^\dagger(\vec{\xi}) \frac{1}{k^2} B[\Sigma(\vec{\xi})] \phi(\vec{\xi}) \right\rangle}, \quad (7)$$

where $\vec{\xi}$ is the phase-space vector and the brackets indicate integration over space, direction, and energy variables.

The k sensitivity for individual cross sections can be obtained from Eq. (7) using the discrete ordinates form of the transport equation. In doing so, the phase-space vector $\vec{\xi}$ has been replaced by indices representing discretization in space, energy, and angle. It has been demonstrated in Ref. 12 that sensitivity coefficients for reaction x , isotope i , energy group g , and computational region z can be represented as

$$S_{k,\Sigma_{x,g,z}^i} = \frac{T_{1,x,g,z}^i + T_{2,g,z}^i + T_{3,x,g,z}^i}{D}, \quad (8)$$

where the denominator D is expressed as

$$D = \frac{1}{k} \sum_{i=1}^I \sum_{z=1}^R V_z \sum_{g=1}^G (\bar{\nu}_{g,z}^i \Sigma_{f,g,z}^i \phi_{g,z}) \sum_{g'=1}^G (\chi_{g',z}^i \phi_{g',z}^\dagger), \quad (9)$$

where

$\chi_{g',z}^i$ = average fraction of fission neutrons emitted into energy group g' from fission of isotope i in region z

$\bar{\nu}_{g,z}^i$ = average number of fission neutrons emitted from fission of isotope i in region z in energy group g

$\Sigma_{f,g,z}^i$ = macroscopic cross section for fission of isotope i in region z and energy group g

I = number of isotopes in the system model

R = number of computational regions in the system model

G = number of neutron energy groups in the system model.

Energy-integrated coefficients are obtained by summing the groupwise coefficients over all energy groups. The T terms of Eq. (8) represent the transport processes for neutron loss, fission production, and scattering to the group of interest in T_1 , T_2 , and T_3 , respectively. The first term is expressed as

$$T_{1,x,g,z}^i = -\Sigma_{x,g,z}^i V_z \sum_{j=0}^{NMOM} (2\ell + 1) \bar{\phi}_{g,z}^{\dagger j} \bar{\phi}_{g,z}^j, \quad (10)$$

where

$\Sigma_{x,g,z}^i$ = macroscopic cross section for some reaction x , of isotope i , energy group g , in region z

ℓ = Legendre order that corresponds to the j 'th real-valued flux moment

$\tilde{\phi}_{g,z}^{\dagger j}$ = j 'th component real-valued adjoint flux moment for energy group g , and region z

$NMOM$ = total number of real-valued flux moments corresponding to the desired Legendre order of expansion.

The second and third terms can be expressed as

$$T_{2,g,z}^i = \frac{1}{k} V_z \bar{v}_{g,z}^i \Sigma_{f,g,z}^i \phi_{g,z} \sum_{g'=1}^G \phi_{g',z}^{\dagger} \chi_{g',z} \quad (11)$$

and

$$T_{3,x,g,z}^i = \sum_{j=0}^{NMOM} V_z \sum_{g'=1}^G \tilde{\phi}_{g',z}^{\dagger j} \tilde{\phi}_{g,z}^j \Sigma_{x,g' \rightarrow g,z}^{\ell,i}, \quad (12)$$

where $\Sigma_{x,g \rightarrow g',z}^{\ell,i}$ is the ℓ 'th moment of the transfer cross section for reaction x of isotope i , from energy group g' to energy group g in region z .

For specific reactions, not all of the T terms defined above are needed to calculate the sensitivity coefficient. The application of Eq. (8) for each type of reaction is outlined as follows:

1. *Capture reaction sensitivity (nonfission, nonscattering)*: Only the $T_{1,x,g,z}^i$ term is used for this class of reactions where $\Sigma_{x,g,z}^i$ is the absorption cross section of interest [(n, γ), (n, α), (n, p), etc.].

2. *Fission reaction sensitivity*: The fission reaction requires $T_{1,x,g,z}^i$ and $T_{2,g,z}^i$, where $\Sigma_{x,g,z}^i$ in the definition of $T_{1,x,g,z}^i$ is the fission cross section.

3. \bar{v} *sensitivity*: The \bar{v} reaction only requires $T_{2,g,z}^i$.

4. χ *sensitivity*: The χ reaction only requires $T_{2,g,z}^i$, with the χ and $\nu \Sigma_f$ terms interchanged.

5. *Scattering reaction sensitivity*: All scattering reactions [elastic, inelastic, and ($n, 2n$) reactions] require $T_{1,x,g,z}^i$ and $T_{3,x,g,z}^i$, where $\Sigma_{x,g,z}^i$ in the definition of $T_{1,x,g,z}^i$ is the scattering cross section and $\Sigma_{x,g' \rightarrow g,z}^{\ell,i}$ in the definition of $T_{3,x,g,z}^i$ is a component of the group-to-group scattering matrix for the ℓ 'th scattering moment of reaction x .

6. *Total reaction sensitivity*: The total reaction requires $T_{1,x,g,z}^i$, $T_{2,g,z}^i$, and $T_{3,x,g,z}^i$. Here, $\Sigma_{x,g,z}^i$ in the definition of $T_{1,x,g,z}^i$ is the total cross section, and $\Sigma_{x,g' \rightarrow g,z}^{\ell,i}$ in the definition of $T_{3,x,g,z}^i$ is a component of the group-to-group scattering matrix for the ℓ 'th scattering moment. For nonfissionable isotopes, $T_{2,g,z}^i$ will be zero.

II.D. Implicit Sensitivity Coefficient Generation

The methodology to calculate the sensitivity coefficients, as presented in Sec. II.C, was developed for fast reactor applications in which the effect of resonance self-shielding in the multigroup cross-section data is minimal. To provide an accurate estimation for systems in which resonance self-shielding is important, the sensitivity coefficients as computed in Eq. (8) require additional terms to account for the first-order implicit effect of perturbations in the material number densities or nuclear data upon the shielded groupwise macroscopic cross-section data. This section reviews techniques developed in Ref. 12 that are applied later in this paper.

The sensitivity of the cross-section data to the input data in turn affects the k_{eff} sensitivities. The implicit portion of the sensitivity coefficient, the sensitivity of the groupwise data to the input quantities, is defined as

$$S_{\Sigma_{x,g}, \omega_i} = \frac{\omega_i}{\Sigma_{x,g}} \frac{\partial \Sigma_{x,g}}{\partial \omega_i}, \quad (13)$$

where ω_i is some input quantity. The ω_i term could represent the number density of a particular material, a certain nuclear data component, or a physical dimension of a system. For the sensitivity coefficients desired, which are the sensitivities of k_{eff} to the groupwise cross-section data, the effect on k_{eff} of perturbing one cross section that affects the resonance-shielded values of all cross sections is the desired result. If ω_i is a certain cross-section data component for process y of nuclide j in energy group h expressed as $\Sigma_{y,h}^j$, which is sensitive to perturbations in process x in energy group g for nuclide i expressed as $\Sigma_{x,g}^i$, the complete sensitivity of k_{eff} due to perturbations of $\Sigma_{x,g}^i$ can be defined using the chain rule for derivatives as

$$\begin{aligned} (S_{k, \Sigma_{x,g}^i})_{total} &= \frac{\Sigma_{x,g}^i}{k} \frac{dk}{d\Sigma_{x,g}^i} = \frac{\Sigma_{x,g}^i}{k} \frac{\partial k}{\partial \Sigma_{x,g}^i} \\ &+ \sum_j \sum_h \frac{\Sigma_{y,h}^j}{k} \frac{\partial k}{\partial \Sigma_{y,h}^j} \times \frac{\Sigma_{x,g}^i}{\Sigma_{y,h}^j} \frac{\partial \Sigma_{y,h}^j}{\partial \Sigma_{x,g}^i} \\ &= S_{k, \Sigma_{x,g}^i} + \sum_j \sum_h S_{k, \Sigma_{y,h}^j} S_{\Sigma_{y,h}^j, \Sigma_{x,g}^i}, \quad (14) \end{aligned}$$

where the sensitivity coefficients with respect to k_{eff} are the explicit components as computed in Eq. (8), with the region subscript z omitted, and j and h are varied to include all processes that are influenced by the value of $\Sigma_{x,g}^i$.

III. IMPLEMENTATION

The methodologies presented in Sec. II of this paper have been implemented into the SCALE code system.

Before detailing this implementation, overviews of current criticality safety analysis capabilities in SCALE, on which the sensitivity analysis tools are based, are presented for the convenience of the reader and to establish a common terminology. A criticality safety analysis with SCALE is performed through an automated execution of a series of computational codes from a single user-defined input. Version 5 of SCALE, SCALE 5, which is under development at this time, has been updated to FORTRAN-90 from the FORTRAN-77 coding of the previous version of SCALE, SCALE 4.4.a. For the first time, SCALE is capable of processing current ENDF/B-VI data-file formats. The individual computational codes in SCALE are referred to as modules. SCALE modules can be of two types: functional and control. A functional module is an individual code that performs a specific computation. A control module guides a computational sequence of a series of functional modules and generates input specific to the individual modules that it executes from a single user-defined sequence input. A control module may be able to perform several different computational sequences, using different functional modules as needed for the type of analysis requested by the user. The Criticality Safety Analysis Sequence (CSAS) control module guides criticality safety analyses in SCALE. Several computational sequences are available within CSAS, but only those relevant to this work are described here.

A CSAS analysis sequence begins with the processing of user-defined materials with the Material Input Processor Library (MIPLIB). MIPLIB prepares a problem-dependent cross-section data library and generates input for the resonance self-shielding codes. Multigroup resonance self-shielding calculations are performed with the BONAMI code in the unresolved resonance region and with the NITAWL-III code in the resolved resonance region. The resonance self-shielding calculations are performed in a user-defined unit-cell geometry for the nuclides present in the problem-dependent cross-section data library. NITAWL-III produces an AMPX working-formatted cross-section data¹³ library in the energy group structure requested by the user. The working library is used in a neutron transport code to perform the criticality calculation. Two multigroup 3-D Monte Carlo neu-

tron transport codes are available in SCALE 5. KENO V.a is a well-established and widely used code that requires geometrical models to consist of primitive bodies, such as cuboids, cylinders, and spheres. KENO-VI is a generalized geometry Monte Carlo code that allows the geometrical model to consist of arbitrarily shaped bodies. Both versions of KENO compute k_{eff} and scalar neutron fluxes, and both operate in forward and adjoint modes. The CSAS25 analysis sequence performs automated criticality safety analyses with KENO V.a. Alternatively, a 1-D deterministic neutron transport calculation can be conducted with XSDRNPM in the CSAS1X analysis sequence. A summary of the SCALE 5 analysis sequences relevant to this work is given in Table I. Brief descriptions of the relevant functional models are given in Table II.

Because it analytically calculates the volumes of user-defined material regions and is more widely used than KENO-VI, KENO V.a was selected for the initial implementation of the sensitivity analysis methodology. First, the methods already present in KENO V.a for the generation of the adjoint flux were tested. Next, the capabilities to calculate the flux moments and angular fluxes were added to KENO V.a. Modifications to calculate the implicit sensitivity coefficient terms were made to the resonance self-shielding codes. A new functional module, the Sensitivity Analysis Module for SCALE (SAMS), was designed to use the forward and adjoint fluxes and the region volume data from KENO V.a along with the problem-dependent cross-section data and the implicit sensitivity coefficient terms to produce the desired sensitivity coefficients. Finally, a new SCALE control module Tools for Sensitivity and Uncertainty Analysis Methodology Implementation in three dimensions (TSUNAMI-3D) was written to perform all steps of the sensitivity calculation in an automated and user-friendly fashion, consistent with the SCALE philosophy.

III.A. Modifications to KENO V.a

Before modifying KENO V.a, investigations were performed to assess the performance of its adjoint solution option. It was noted that for certain classes of problems, particularly fast systems, it was necessary to

TABLE I
Relevant Control Sequences in SCALE 5

Control Sequence	Material Input	Functional Modules Executed by the Control Sequence					
CSAS1X	MIPLIB	BONAMI	NITAWL-III	XSDRNPM			
CSAS25	MIPLIB	BONAMI	NITAWL-III		KENO V.a		
TSUNAMI-3D-K5N	MIPLIB	BONAMI	NITAWL-III		KENO V.a	KENO V.a	SAMS
					Adjoint	Forward	
TSUNAMI-3D-K5	MIPLIB/SENLIB	BONAMIST	NITAWLST		KENO V.a	KENO V.a	SAMS
					Adjoint	Forward	

TABLE II
Relevant Functional Modules in SCALE 5

Functional Module	Brief Description
BONAMI	Existing SCALE functional module that performs resonance self-shielding calculations in the unresolved resonance region.
BONAMIST	New enhanced version of BONAMI that performs resonance self-shielding calculations in the unresolved resonance region and generates the sensitivities of the self-shielded groupwise cross sections to the input data.
NITAWL-III	Existing SCALE functional module that performs resonance self-shielding calculations in the resolved resonance regions. Able to process ENDF/B-VI cross-section data files.
NITAWLST	New enhanced version of NITAWL-II that performs resonance self-shielding calculations in the resolved resonance region and generates the sensitivities of the self-shielded groupwise cross sections to the input data.
XSDRNPM	Existing 1-D deterministic neutron transport code that operates as a functional module within SCALE.
KENO V.a	Existing 3-D Monte Carlo neutron transport code that operates as a functional module within SCALE. Flux moment and angular flux calculational techniques were added to KENO V.a as part of this current research.
SAMS	New SCALE functional module that generates the sensitivity of k_{eff} computed by a neutron transport code to the cross-section data used in the transport calculation.

significantly increase the number of histories per generation to prevent all histories from being terminated by Russian roulette before they produced a new set of fission points for the next generation. If no fission points are created by a generation of particles, the code prints an error message and ceases execution. For example, in an adjoint calculation of the GODIVA experiment,¹⁴ which consists of a bare sphere of highly enriched uranium metal, the number of histories per generation must be set to at least 15 000 to ensure that some fission points are created in each generation. In moderated systems, the number of histories per generation typically is several hundred to a few thousand. Methods for biasing the adjoint solution to obtain better performance have been

investigated; at this point, however, these methods have not been implemented.

The calculation of the flux moments required the calculation of the center of the fuel regions in KENO V.a to establish a reference point for the transformed coordinate system as discussed in Sec. II.A. A methodology was developed to analytically determine the center of the fueled regions from the geometry description. This methodology is equivalent to a center-of-mass calculation with a uniform density for fissile materials and a zero density for all other materials. Other options are available for the user to input the desired center reference point from which the flux moments are calculated. The ability to specify a region-dependent reference point for the flux moment calculations is especially useful for systems with loosely coupled individual components, where the moments calculated in reference to the center of the entire system do not accurately represent the moments of each component.

New routines were written to perform the coordinate transform and calculate the spherical harmonics functions or angular quadrature direction for each history. Depending on whether the user desires flux moments and/or angular fluxes, calls to these routines are made at each point where a flux tally occurs. To ensure that the angular-dependent tallies are precise, the tallies are made at five points along the particle's track since the last tally. The multiple-tally procedure is necessary because the angle between the direction of travel and the position vector, measured relative to the center of the fueled regions, can change significantly over the length of a given track. The use of five tally points was arrived at through an interactive process to optimize the results. For adjoint problems, the fluxes are determined for the reflected angle from the direction of travel. An input parameter was added to allow the selection of the Legendre order through which the flux moments are calculated. This parameter does not affect the scattering order used by KENO V.a in the calculation of collisions. A separate parameter was also added to select the order of the quadrature set for the angular flux calculations.

The flux moment calculations are conducted as shown in Sec. II.A. The angular flux calculations, described in Sec. II.B, are more complex. For this implementation, symmetric-level-quadrature sets are used for consistency with deterministic S_n codes.¹⁵ The quadrature direction in which the particle is traveling is determined by comparing the direction cosines of the particle, in the transformed coordinate system, against the range of a given quadrature direction.

Because the particles' directions are assigned from a continuum, a methodology was devised to determine the quadrature direction in which the particle is traveling. Through this methodology, the quadrature direction is assigned based on the proximity of a particle's direction of travel to a discrete angle in the quadrature set. To ensure that a given particle can only be assigned to one

region, the solid angles representing $d\hat{\Omega}$ are assigned such that they sweep out equal volumes of a unit sphere without overlapping. The octant in which the particle is traveling is determined first, and then the region within that octant is determined based on the order of the quadrature set.

As an illustration of this technique, an example for an S_4 quadrature set is presented. For angular flux calculations, the directional space is divided into octants, which are sequenced for consistency with deterministic S_n codes as shown in Table III. Here, μ , η , and ξ take on their ordinary meanings as direction cosines with the x , y , and z axes, respectively.

A sketch of the symmetric level quadrature for the S_4 set for the first octant is shown in Fig. 2. In deterministic neutron transport, the solution would be computed for directions corresponding to the labels 1, 2, and 3. However, in Monte Carlo transport, the particles can travel in any direction, not just discrete directions. The particle must be tallied in the quadrature direction corresponding to the particle's direction of travel. The selection of the quadrature direction is illustrated by the hatched surfaces shown in Fig. 3. A particle will be counted in the first subregion if its ξ value is greater than ξ_2 , shown as the horizontally hatched surface in Fig. 3. A particle will be counted in the second subregion if its ξ value is less than ξ_2 and its μ value is greater than μ_2 , shown as the vertically hatched surface in Fig. 3. A particle will be counted in the third subregion if its ξ value is less than ξ_2 and its μ value is less than μ_2 , shown as the diagonally hatched surface in Fig. 3. The values of μ_2 and ξ_2 are chosen such that the solid angles with surfaces corresponding to each of the hatched surfaces sweep out equal volumes of a unit sphere. Because the scalar flux tally is divided among all of the angles in the quadrature set, a weight of 1.0 is assigned to each direction. With this weight, the scalar flux can be reconstructed by simply adding the fluxes from each angular flux direction. Using the techniques defined in the S_4 quadrature set example, angular flux calculation techniques have been implemented for even-numbered quadrature sets up to S_{16} .

TABLE III

Sequencing of Octants for Angular Flux Calculations

Octant Index	Sign of μ	Sign of η	Sign of ξ
1	+	+	+
2	+	-	+
3	-	-	+
4	-	+	+
5	+	+	-
6	+	-	-
7	-	-	-
8	-	+	-

III.B. Calculation of Implicit Sensitivity Coefficients

The calculations of the implicit components of the sensitivity coefficients are performed by enhanced versions of the resonance processing codes, as well as enhanced routines in MIPLIB. To simplify the generation

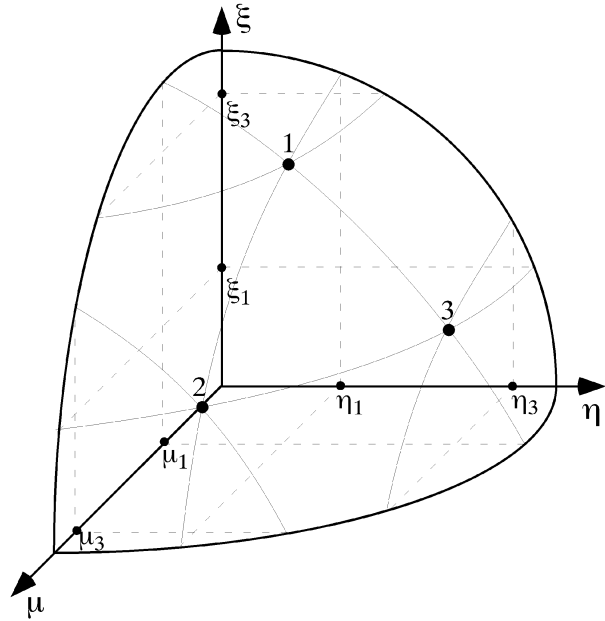


Fig. 2. Symmetric level S_4 quadrature arrangement for the first octant.

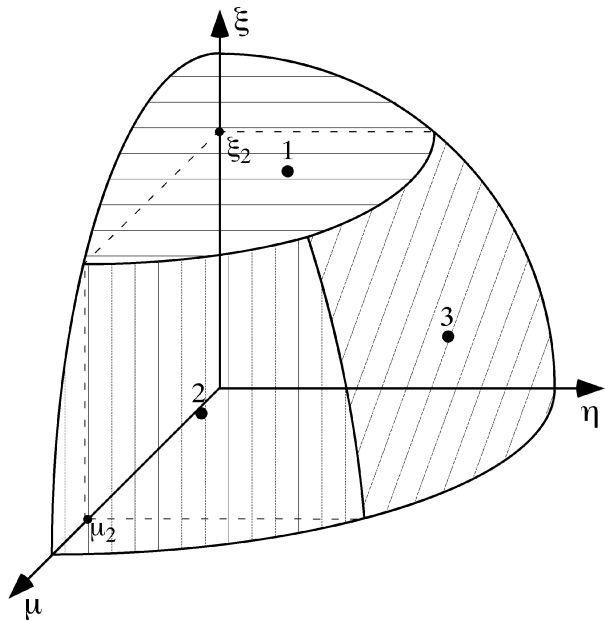


Fig. 3. Surfaces corresponding to each direction in octant one for S_4 quadrature set.

of the required implicit sensitivities, the GRESS automatic differentiation program¹⁶ was used to process the appropriate source code such that the enhanced versions of the codes compute the same quantities as the standard codes as well as the sensitivities of these quantities to the input data. Because GRESS is limited to processing only FORTRAN-77 coding, and SCALE 5 is programmed in FORTRAN-90, versions of the necessary codes from SCALE 4.4.a, which is programmed in FORTRAN-77, were used for this exercise. Where possible, any new capabilities in SCALE 5 were added to the SCALE 4.4.a codes. One important omission is that NITAWL-III from SCALE 5 can process multipole formatted resolved resonance parameters from ENDF/B-VI data, but NITAWL-II from SCALE 4.4.a does not have this capability. Thus, the implicit sensitivity coefficients can only be generated from ENDF/B-V and earlier cross-section data.

The Dancoff factors necessary for the resonance self-shielding calculations are computed by MIPLIB and passed as input to BONAMI and NITAWL-III. Lumped moderator scattering cross sections are also computed by MIPLIB and passed as input to NITAWL-III. GRESS was used to process the appropriate MIPLIB routines to generate the sensitivity of the Dancoff factors and lumped moderator scattering cross sections to the input material number densities. The GRESS-enhanced MIPLIB routines are called SENLIB. The GRESS-enhanced versions of BONAMI and NITAWL-II have been named BONAMIST and NITAWLST, respectively. For BONAMIST, the sensitivities of the shielded groupwise cross sections in the unresolved resonance region are computed with respect to the input material number densities and the Dancoff factors for each material region. NITAWLST computes the sensitivity of the groupwise shielded cross sections in the resolved resonance region to the scattering cross section of the lumped moderators and the Dancoff factors for each nuclide. The sensitivities are stored on formatted file output by each code. The resonance self-shielded cross-section data library produced by the GRESS-enhanced codes is identical to one that would have been produced by the corresponding nonenhanced codes.

III.C. Sensitivity Analysis Module for SCALE (SAMS)

The SAMS module was designed to execute under the SCALE driver in conjunction with the other functional modules of the SCALE code system. SAMS uses either the flux moments or angular fluxes generated from the enhanced version of KENO V.a along with the problem-dependent cross-section data file to produce the explicit sensitivity coefficients using the methodology presented in Sec. II.C. The number of particle histories or generations from the Monte Carlo calculations is only used for statistical uncertainty analyses, and different

numbers of histories are permitted in the forward and adjoint cases. SAMS automatically checks for available data in the cross-section data file and prepares a list of sensitivity coefficients that can be calculated for each nuclide. SAMS then calculates the sensitivity coefficients and their associated Monte Carlo uncertainties for each nuclide for each region containing that nuclide on a groupwise basis. Once all of the groupwise sensitivity coefficients have been calculated, they are summed to produce energy- and region-integrated sensitivity coefficients and their associated Monte Carlo uncertainties.

Subsequent to the computation of the explicit portion of the sensitivity coefficients, data from SENLIB, BONAMIST, and NITAWLST are used to compute the implicit portion of the sensitivity coefficients. This implementation of the implicit sensitivity coefficients is more general than that presented in the example calculation of Ref. 12, as it allows for the assessment of the implicit components for all reactions due to interaction with all nuclides. Because the sensitivity of a response to a material number density is equivalent to the sensitivity of the same response to the corresponding total macroscopic cross section, the computation of the implicit sensitivity coefficients can be based on the sensitivity to the input material number densities. The implicit effect of the number densities on k_{eff} must be accounted for from several sources. One source is the effect of the number densities' input to BONAMIST on the shielded cross sections in the unresolved resonance region. For this case, the implicit sensitivity of k_{eff} to the total cross section of nuclide i is

$$\begin{aligned} (S_{k, \Sigma_{T,g}^i})_{implicit} &= \sum_j \sum_y \sum_h \frac{\Sigma_{y,h}^j}{k} \frac{\partial k}{\partial \Sigma_{y,h}^j} \times \frac{\Sigma_T^i}{\Sigma_{y,h}^j} \frac{\partial \Sigma_{y,h}^j}{\partial \Sigma_T^i} \\ &\times \frac{\Sigma_{T,g}^i}{\Sigma_T^i} \frac{\partial \Sigma_T^i}{\partial \Sigma_{T,g}^i} \\ &= \sum_j \sum_y \sum_h S_{k, \Sigma_{y,h}^j} S_{\Sigma_{y,h}^j, \Sigma_T^i} S_{\Sigma_T^i, \Sigma_{T,g}^i} \\ &= \sum_j \sum_y \sum_h S_{k, \Sigma_{y,h}^j} S_{\Sigma_{y,h}^j, N^i} S_{\Sigma_T^i, \Sigma_{T,g}^i}, \quad (15) \end{aligned}$$

where j and y are varied to include all processes that are sensitive to N^i , the number density of the i 'th nuclide. Additionally, the energy group for the implicit sensitivity g is varied over all energies. The sensitivity of the total macroscopic cross section to the groupwise macroscopic total cross section $S_{\Sigma_T^i, \Sigma_{T,g}^i}$ is simply 1.0. For data computed by SENLIB and input to BONAMIST and NITAWLST, an additional term is necessary to account for the sensitivity of the SENLIB parameter, denoted ω_m . The chain rule for derivatives can again be used to propagate this sensitivity to a k_{eff} sensitivity. The implicit sensitivity of k_{eff} to the input number densities, in this case, is

$$\begin{aligned}
(S_{k, \Sigma_{T,g}^i})_{implicit} &= \sum_m \sum_j \sum_y \sum_h \frac{\Sigma_{y,h}^j}{k} \frac{\partial k}{\partial \Sigma_{y,h}^j} \times \frac{\omega_m}{\Sigma_{y,h}^j} \frac{\partial \Sigma_{y,h}^j}{\partial \omega_m} \\
&\times \frac{\Sigma_T^i}{\omega_m} \frac{\partial \omega_m}{\partial \Sigma_T^i} \times \frac{\Sigma_{T,g}^i}{\Sigma_T^i} \frac{\partial \Sigma_T^i}{\partial \Sigma_{T,g}^i} \\
&= \sum_m \sum_j \sum_y \sum_h S_{k, \Sigma_{y,h}^j} S_{\Sigma_{y,h}^j, \omega_m} S_{\omega_m, \Sigma_T^i} S_{\Sigma_T^i, \Sigma_{T,g}^i} \\
&= \sum_m \sum_j \sum_y \sum_h S_{k, \Sigma_{y,h}^j} S_{\Sigma_{y,h}^j, \omega_m} \\
&\times S_{\omega_m, N^i} S_{\Sigma_T^i, \Sigma_{T,g}^i}, \quad (16)
\end{aligned}$$

where m is varied to include all SENLIB-computed parameters that use the material number densities in their calculation and are input to BONAMIST and NITAWLST.

The calculation of the implicit sensitivity of a total cross-section component in the unresolved resonance region requires the sum of the implicit quantities computed in Eqs. (15) and (16) with ω_m varied to include the Dancoff factor for each zone used in the BONAMIST calculation. The calculation of the implicit sensitivity of a total cross-section component in the resolved resonance region requires only the use of Eq. (16) with ω_m varied to include the Dancoff factor as well as the lumped scattering parameters for each material input to NITAWLST. Because a single implicit sensitivity depends on numerous other sensitivities, a particular implicit sensitivity can have contributions from both the resolved and unresolved resonance regions. Thus, all sensitivity data computed from SENLIB, BONAMIST, and NITAWLST must be checked for contributions to the implicit sensitivity of interest.

To compute the implicit portion of sensitivity coefficients for reactions x other than total, an additional term must be employed. With the implicit sensitivity of k_{eff} to the total cross section computed, the chain rule for derivatives is again applied to propagate the sensitivity of k_{eff} to the total cross section to the sensitivity of k_{eff} to some other process. This is accomplished using the sensitivity of the total cross section to the particular processes, computed from the unshielded cross-section data as

$$(S_{k, \Sigma_{x,g}^i})_{implicit} = \left(\frac{\Sigma_{T,g}^i}{k} \frac{\partial k}{\partial \Sigma_{T,g}^i} \right)_{implicit} \times \left(\frac{\Sigma_{x,g}^i}{\Sigma_{T,g}^i} \frac{\partial \Sigma_{T,g}^i}{\partial \Sigma_{x,g}^i} \right). \quad (17)$$

With the implicit sensitivities properly computed, the complete sensitivity coefficient by group can be computed as the sum of the explicit and implicit terms as

$$(S_{k, \Sigma_{x,g}^i})_{total} = (S_{k, \Sigma_{x,g}^i})_{explicit} + (S_{k, \Sigma_{x,g}^i})_{implicit}. \quad (18)$$

The Monte Carlo uncertainties in the forward and adjoint flux solutions and the value of k_{eff} are propagated to the final sensitivity results using standard error propagation techniques.¹⁷ The forward and adjoint fluxes are treated as uncorrelated to each other. Also, the groupwise values of each flux solution are treated as uncorrelated. The flux moments within each group are treated as fully correlated. Although this method provides an adequate assessment of the statistical uncertainty in the sensitivity coefficients, a more robust technique may be implemented in subsequent revisions.

The sensitivity coefficients and their associated Monte Carlo uncertainties integrated over energy and region for every nuclide and reaction are written to an output file. A data file containing the groupwise sensitivity data for every nuclide and reaction is also produced for use in subsequent postprocessing or plotting.

Furthermore, SAMS can use cross-section-covariance data files to propagate the uncertainties in the cross-section data to an uncertainty in the computed k_{eff} value of the system analyzed. An explanation of the cross-section-covariance data file and a theoretical development of this uncertainty propagation are given in a companion paper.⁴

III.D. TSUNAMI-3D SCALE Control Module

The TSUNAMI-3D control module for SCALE was designed to allow automated use of the 3-D sensitivity techniques with Monte Carlo methods. Two analysis sequences developed within the TSUNAMI-3D control module, TSUNAMI-3D-K5N and TSUNAMI-3D-K5, are described here. The available analysis sequences are detailed in Table I. The relevant functional modules are described in Table II. The TSUNAMI-3D-K5N analysis sequence performs Monte Carlo calculations using the enhanced version of KENO V.a and then calculates sensitivity data with the SAMS module. TSUNAMI-3D-K5N performs resonance self-shielding calculations with the standard BONAMI and NITAWL-III codes currently under development for SCALE 5. The TSUNAMI-3D-K5N analysis sequence allows the use of ENDF/B-VI cross-section data but does not calculate the implicit terms of the sensitivity coefficients. The TSUNAMI-3D-K5 analysis sequence computes the implicit portion of the sensitivity coefficients by replacing some routines from MIPLIB with corresponding routines from SENLIB, BONAMI with BONAMIST, and NITAWL-III with NITAWLST. The same unit-cell types available with CSAS25 are available in TSUNAMI-3D-K5N and TSUNAMI-3D-K5. In addition to the usual problem-dependent cross-section data library, the master sensitivity library is produced by NITAWL-III or NITAWLST. This library contains additional reaction-dependent scattering data not available in the commonly used working-format library. After the chosen resonance

processing is completed, the TSUNAMI-3D control module then executes an adjoint criticality calculation with the enhanced version of KENO V.a, which calculates the angular fluxes or flux moments, and stores these data in a binary data file. Subsequent to the adjoint calculation, TSUNAMI-3D executes the corresponding forward calculation with KENO V.a and stores the required data in a separate binary data file. After generating the required data files, TSUNAMI-3D executes the SAMS module to produce the sensitivity coefficients. A flow diagram of the TSUNAMI-3D-K5N and TSUNAMI-3D-K5 analysis sequences is shown in Fig. 4.

For the convenience of the user, the TSUNAMI-3D-K5N and TSUNAMI-3D-K5 analysis sequences were designed to use input very similar to CSAS25. In fact, if the default parameters for the adjoint calculation and sensitivity coefficient generation are acceptable, the required input is exactly the same as that required by CSAS25. Several new optional input parameters have been added for the flux moment and angular flux calculations, the adjoint calculation, and the execution of the SAMS module. These will be described in detail with the code documentation and user's guide, which will be issued with SCALE 5.

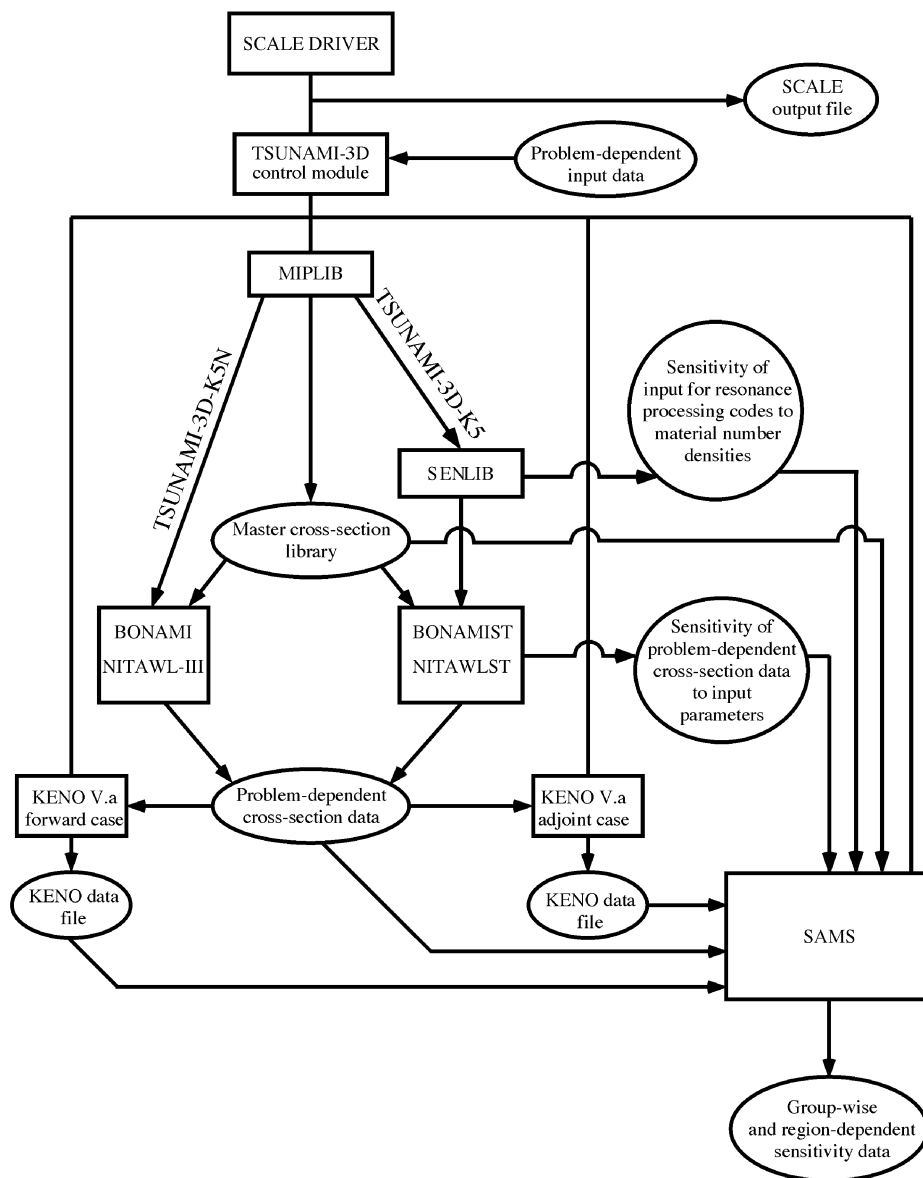


Fig. 4. Flow diagram for the TSUNAMI-3D SCALE control module.

IV. SAMPLE CALCULATIONS

Sensitivity results calculated with TSUNAMI-3D have been verified by comparison with sensitivity results generated by direct perturbation of the input quantities. For each input quantity examined by direct perturbation, the k_{eff} of the system was computed first with the nominal values of the input quantities, then with a selected input value increased by a certain percentage, and then with the value decreased by the same percentage. The direct perturbation sensitivity coefficient of k_{eff} to some input value α is computed as

$$S_{k,\alpha} = \frac{\alpha}{k} \times \frac{dk}{d\alpha} = \frac{\alpha}{k} \times \frac{k_{\alpha^+} - k_{\alpha^-}}{\alpha^+ - \alpha^-}, \quad (19)$$

where α^+ and α^- represent the increased and decreased values of the input quantity α , respectively, and k_{α^+} and k_{α^-} represent the corresponding values of k_{eff} .

IV.A. $U(2)F_4$ Test Case

A simple test case was analyzed through direct perturbation methods as well as with TSUNAMI-3D, and the results were compared. The selected sample problem, which is identical to the test case selected for the validation of the 1-D SEN1 sensitivity analysis sequence,⁶ is based on an unreflected rectangular parallelepiped consisting of a homogeneous mixture UF_4 and paraffin with an enrichment of 2% in ^{235}U . The H/ ^{235}U atomic ratio is 293.9:1. The dimensions of the experiment¹⁸ were $56.22 \times 56.22 \times 122.47$ cm. For consistency with the previous SEN1 analysis and ease of obtaining precise direct perturbation results, this experiment was modeled as a sphere with a critical radius of 38.50 cm.

Direct perturbation results were obtained using the 1-D criticality analysis sequence,⁵ CSAS1X, of SCALE. To obtain the direct perturbation results shown in Table IV, 11 independent criticality calculations were performed. First, the baseline k_{eff} was computed using the actual input values. Next, the number density of a single nuclide was increased by 5%, and the k_{eff} was recomputed. The same number density was then decreased by 5% from the baseline value, and the k_{eff} was recomputed. With the three values computed, Eq. (19) was used to compute the sensitivity of k_{eff} to the material number density, which is equivalent to the sensitivity of k_{eff} to the total cross section. The perturbed calculations were conducted for each nuclide in the problem description.

This experiment was modeled as a single computational region with TSUNAMI-3D-K5 using the angular flux calculation option with an S_{10} quadrature set and the 44-group ENDF/B-V SCALE library. Flux moments were expanded to third order in the SAMS module. The number of particles per generation was set at 5000 with 1000

generations for the forward case. TSUNAMI-3D-K5 automatically increases the number of particles per generation by a factor of 3 for the adjoint analysis. These results, shown in Table IV, indicate similarity with the direct perturbation results for some nuclides, but not for others. Differences outside of 1σ vary from 1.2% for ^{235}U to 33% for C. A subsequent analysis was performed with the TSUNAMI-3D-K5 model divided into nine spherical shells, with all other parameters held constant. The results from this analysis, also shown in Table IV, compare much more favorably with the direct perturbation results. For this model, the maximum difference outside 1σ is for ^{235}U and is 1.8%. In subsequent calculations with only a $\pm 2\%$ variation in the ^{235}U number density, a direct perturbation sensitivity value of 0.252 was obtained, which is equivalent to the result obtained with TSUNAMI-3D-K5, indicating that for ^{235}U , a $\pm 5\%$ variation could have produced a nonlinear response.

The differences in the results from the two TSUNAMI-3D models, one region and nine regions, are due to the summation of the product of the forward and adjoint fluxes over the regions in the problem. For a region in which the flux moments vary greatly by position, subdividing will provide better resolution of the variation of the flux across the system and produce more accurate results. The number of regions necessary for accurate computation of the sensitivity coefficients was determined through an iterative process. Models divided into more regions produce the same results as the nine-region model. It should be noted that increasing the number of computational regions increases the run time for this problem by $\sim 10\%$. The sensitivity results from the nine-region model using the TSUNAMI-3D-K5N analysis sequence, which does not include the contributions from the implicit sensitivity coefficients, are also shown in Table IV. The TSUNAMI-3D-K5N analysis was performed with the same 44-group ENDF/B-V library as was used in the TSUNAMI-3D-K5 analysis. The differences in the computed results between TSUNAMI-3D-K5N and TSUNAMI-3D-K5 for the same system model are $\sim 20\%$ for 1H and nearly 40% for ^{238}U . Thus, the use of the TSUNAMI-3D-K5 sequence is strongly recommended over the use of the TSUNAMI-3D-K5N sequence. However, TSUNAMI-3D-K5N should produce accurate results for fast systems where resonance self-shielding is not important.

To further verify the sensitivity data from the TSUNAMI-3D sequences, groupwise sensitivity coefficients were computed for 1H elastic scattering with direct perturbation techniques. To accomplish this, the 1-D scattering data as well as the 2-D scattering matrix for 1H were perturbed on a groupwise basis in the master cross-section data library using the AMPX utility module¹³ CLAROL. Furthermore, as the scattering cross sections for 1H were perturbed, the lumped moderator scattering data input to NITAWL was appropriately perturbed on a groupwise basis. This exercise was carried

TABLE IV

Energy-Integrated Sensitivities and Standard Deviations for Spherical Models of U(2)F₄ Test Case
for Direct Perturbation and TSUNAMI-3D Models

Isotope	Reaction	Direct Perturbation	TSUNAMI-3D-K5 (Single Computational Region) $k_{eff} = 1.00373 \pm 0.00041$	TSUNAMI-3D-K5 (Nine Computational Regions) $k_{eff} = 1.00416 \pm 0.00037$	TSUNAMI-3D-K5N (Nine Computational Regions) $k_{eff} = 1.00332 \pm 0.00035$
¹ H	Total	2.26E-01 ^a	2.43E-01 ± 6.19E-03	2.24E-01 ± 6.23E-03	2.90E-01 ± 6.33E-03
¹ H	Scatter		3.43E-01 ± 6.17E-03	3.26E-01 ± 6.19E-03	3.92E-01 ± 6.29E-03
¹ H	Elastic		3.43E-01 ± 6.17E-03	3.26E-01 ± 6.19E-03	3.92E-01 ± 6.29E-03
¹ H	Capture		-1.00E-01 ± 4.93E-05	-1.02E-01 ± 5.01E-05	-1.02E-01 ± 5.09E-05
¹ H	<i>n, γ</i>		-1.00E-01 ± 4.93E-05	-1.02E-01 ± 5.01E-05	-1.02E-01 ± 5.09E-05
¹² C	Total	2.51E-02	3.38E-02 ± 3.86E-04	2.49E-02 ± 3.65E-04	3.18E-02 ± 3.70E-04
¹² C	Scatter		3.45E-02 ± 3.85E-04	2.56E-02 ± 3.65E-04	3.25E-02 ± 3.70E-04
¹² C	Elastic		3.42E-02 ± 3.85E-04	2.53E-02 ± 3.64E-04	3.22E-02 ± 3.70E-04
¹² C	<i>n, n'</i>		2.56E-04 ± 7.26E-06	2.46E-04 ± 4.73E-06	2.47E-04 ± 4.79E-06
¹² C	Capture		-6.68E-04 ± 1.63E-06	-6.71E-04 ± 1.05E-06	-6.70E-04 ± 1.07E-06
¹² C	<i>n, γ</i>		-4.93E-04 ± 2.41E-07	-4.99E-04 ± 2.45E-07	-4.99E-04 ± 2.49E-07
¹² C	<i>n, p</i>		-3.18E-08 ± 4.42E-10	-3.10E-08 ± 2.80E-10	-3.09E-08 ± 2.86E-10
¹² C	<i>n, d</i>		-8.03E-08 ± 1.12E-09	-7.85E-08 ± 7.08E-10	-7.81E-08 ± 7.24E-10
¹² C	<i>n, α</i>		-1.75E-04 ± 1.61E-06	-1.72E-04 ± 1.02E-06	-1.71E-04 ± 1.04E-06
¹⁹ F	Total	3.99E-02	5.32E-02 ± 5.73E-04	3.95E-02 ± 4.89E-04	4.75E-02 ± 4.95E-04
¹⁹ F	Scatter		5.88E-02 ± 5.71E-04	4.50E-02 ± 4.87E-04	5.30E-02 ± 4.93E-04
¹⁹ F	Elastic		4.03E-02 ± 4.03E-04	2.93E-02 ± 3.70E-04	3.72E-02 ± 3.76E-04
¹⁹ F	<i>n, n'</i>		1.85E-02 ± 2.32E-04	1.58E-02 ± 1.85E-04	1.58E-02 ± 1.87E-04
¹⁹ F	<i>n, 2n</i>		3.34E-06 ± 4.25E-08	3.28E-06 ± 2.84E-08	3.27E-06 ± 2.91E-08
¹⁹ F	Capture		-5.54E-03 ± 9.02E-06	-5.53E-03 ± 5.93E-06	-5.51E-03 ± 5.97E-06
¹⁹ F	<i>n, γ</i>		-2.31E-03 ± 1.05E-06	-2.34E-03 ± 1.05E-06	-2.33E-03 ± 1.06E-06
¹⁹ F	<i>n, p</i>		-2.22E-04 ± 1.07E-06	-2.18E-04 ± 6.77E-07	-2.16E-04 ± 6.86E-07
¹⁹ F	<i>n, d</i>		-1.09E-05 ± 1.14E-07	-1.06E-05 ± 7.25E-08	-1.06E-05 ± 7.41E-08
¹⁹ F	<i>n, t</i>		-2.39E-06 ± 3.31E-08	-2.34E-06 ± 2.10E-08	-2.33E-06 ± 2.15E-08
¹⁹ F	<i>n, α</i>		-3.00E-03 ± 8.16E-06	-2.96E-03 ± 5.34E-06	-2.94E-03 ± 5.37E-06
²³⁵ U	Total	2.57E-01	2.60E-01 ± 3.80E-04	2.52E-01 ± 3.78E-04	2.52E-01 ± 3.83E-04
²³⁵ U	Scatter		5.39E-04 ± 2.94E-06	4.17E-04 ± 2.46E-06	4.50E-04 ± 2.49E-06
²³⁵ U	Elastic		3.57E-04 ± 1.91E-06	2.53E-04 ± 1.86E-06	2.85E-04 ± 1.89E-06
²³⁵ U	<i>n, n'</i>		1.74E-04 ± 1.86E-06	1.56E-04 ± 1.42E-06	1.57E-04 ± 1.43E-06
²³⁵ U	<i>n, 2n</i>		1.11E-05 ± 6.15E-08	1.10E-05 ± 4.20E-08	1.09E-05 ± 4.28E-08
²³⁵ U	Fission		3.70E-01 ± 3.42E-04	3.64E-01 ± 3.33E-04	3.64E-01 ± 3.38E-04
²³⁵ U	Capture		-1.11E-01 ± 4.94E-05	-1.12E-01 ± 5.02E-05	-1.12E-01 ± 5.10E-05
²³⁵ U	<i>n, γ</i>		-1.11E-01 ± 4.94E-05	-1.12E-01 ± 5.02E-05	-1.12E-01 ± 5.10E-05
²³⁵ U	Nubar		9.49E-01 ± 1.85E-04	9.49E-01 ± 7.18E-05	9.50E-01 ± 6.81E-05
²³⁵ U	Chi		9.49E-01 ± 2.07E-04	9.50E-01 ± 8.03E-05	9.50E-01 ± 7.62E-05
²³⁸ U	Total	-2.07E-01	-1.96E-01 ± 2.70E-04	-2.06E-01 ± 2.34E-04	-2.88E-01 ± 2.29E-04
²³⁸ U	Scatter		6.85E-02 ± 1.66E-04	6.23E-02 ± 1.28E-04	2.77E-02 ± 1.27E-04
²³⁸ U	Elastic		5.35E-02 ± 7.87E-05	4.88E-02 ± 7.24E-05	1.41E-02 ± 7.06E-05
²³⁸ U	<i>n, n'</i>		1.39E-02 ± 1.30E-04	1.24E-02 ± 9.72E-05	1.25E-02 ± 9.79E-05
²³⁸ U	<i>n, 2n</i>		1.03E-03 ± 7.62E-06	1.01E-03 ± 5.21E-06	1.01E-03 ± 5.31E-06
²³⁸ U	Fission		3.46E-02 ± 2.46E-05	3.38E-02 ± 1.79E-05	3.37E-02 ± 1.80E-05
²³⁸ U	Capture		-3.01E-01 ± 1.64E-04	-3.04E-01 ± 1.58E-04	-3.50E-01 ± 1.54E-04
²³⁸ U	<i>n, γ</i>		-3.01E-01 ± 1.64E-04	-3.04E-01 ± 1.58E-04	-3.50E-01 ± 1.54E-04
²³⁸ U	Nubar		5.38E-02 ± 1.30E-05	5.29E-02 ± 5.06E-06	5.05E-02 ± 4.62E-06
²³⁸ U	Chi		5.14E-02 ± 1.12E-05	5.05E-02 ± 4.26E-06	5.05E-02 ± 4.04E-06

^aRead as 2.26×10^{-1} .

out with +5% and -5% cross-section perturbations for each energy group in the 44-group SCALE ENDF/B-V library structure. BONAMI, NITAWL-III, and XSDRNPM were then used to compute the k_{eff} of the system with each perturbed library. The groupwise sensitivity coefficients were then computed using Eq. (19). The results from this direct perturbation analysis as well as the TSUNAMI-3D-K5N and TSUNAMI-3D-K5 results from the nine-region models are shown as sensitivity profiles in Fig. 5. The TSUNAMI-3D-K5 results provide excellent agreement with the direct perturbation results. Because of their similarity, the TSUNAMI-3D-K5 results are difficult to discern from the direct perturbation results in Fig. 5. The effect of omitting the contribution of the implicit sensitivity coefficients in the TSUNAMI-3D-K5N model can be seen in the difference between the TSUNAMI-3D-K5N and TSUNAMI-3D-K5 results. In particular, the implicit effect of the large resonance in ^{238}U capture at 6.7 eV on the ^1H elastic scattering sensitivity profile is clearly shown in the difference between the TSUNAMI-3D-K5 and TSUNAMI-3D-K5N results. Without the implicit effects, the sensitivity in the energy group including 6.7 eV is overestimated by a factor of nearly 2. Also shown in the legend of Fig. 5 are the energy-integrated values, noted with a , and the sum of the negative values, noted with osc , for each sensitivity profile. Thus, for ^1H elastic scattering, the TSUNAMI-3D-K5 energy-integrated

value of 0.3257 ± 0.0063 is statistically equivalent to the direct perturbation value of 0.3223.

The execution time for a criticality analysis of the nine-region model using the CSAS25 analysis sequence in the forward calculational mode on a Compaq XP1000 workstation required 10.32 min, including the resonance self-shielding and criticality calculations. The analysis of the same model in the TSUNAMI-3D-K5 sensitivity analysis sequence required 98.75 min, including the resonance shielding, forward and adjoint criticality, and sensitivity calculations. Thus, a factor of ~ 10 is required to move from the computation of the system k_{eff} value and scalar fluxes in CSAS25, to the generation of these parameters plus the sensitivity of k_{eff} to every reaction of every nuclide for every region in the system. For this test case, a total of 45 sensitivity profiles were calculated for each region of the system in addition to the total for all regions. In this 44-group energy structure, there are 1980 data points for each region, making a total of 17820 unique sensitivity coefficients. The generation of these same sensitivity coefficients through direct perturbation techniques would require 35641 criticality calculations that require 10.32 min each for code execution. This does not include the substantial time required to generate appropriate inputs. The execution time alone would require >6000 h, where TSUNAMI-3D-K5 performs the complete analysis in <100 min.

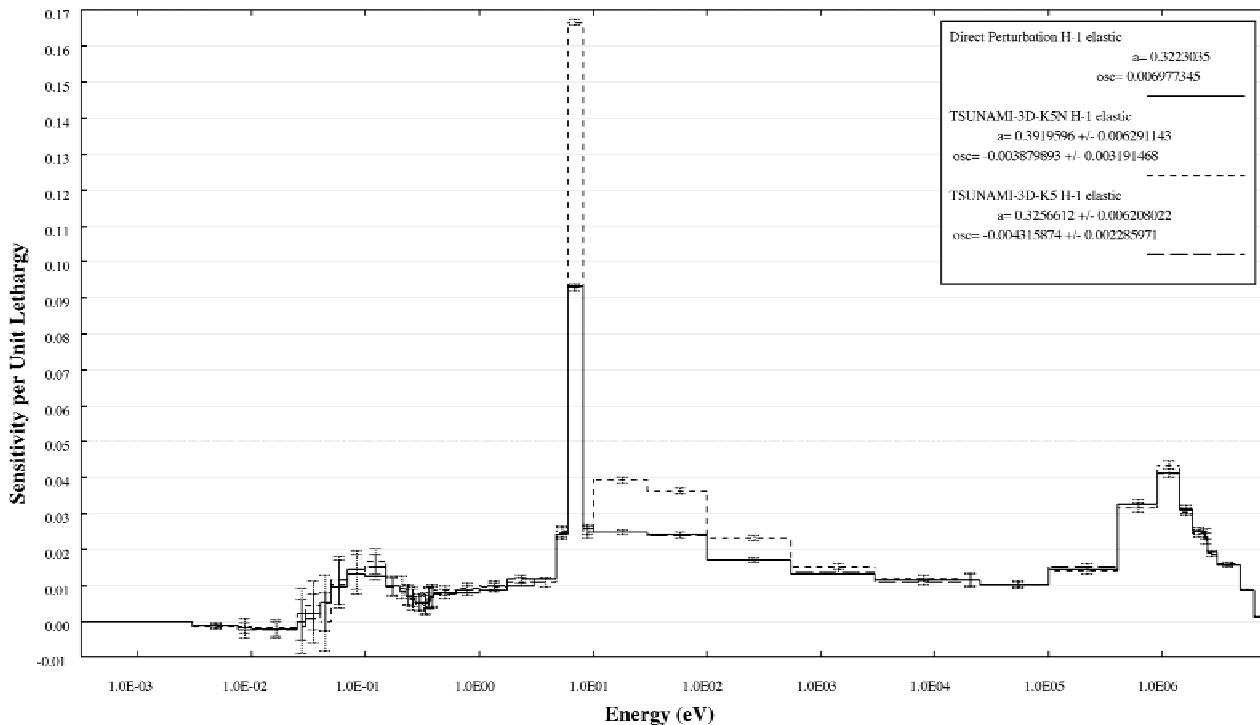


Fig. 5. Comparison of elastic scattering sensitivity profiles for ^1H from $\text{U}(2)\text{F}_4$ test case.

IV.B. SHEBA-II Test Case

To verify the accuracy of the TSUNAMI-3D calculations for a more complex geometrical configuration, a sensitivity analysis of the SHEBA-II experiment^{19,20} was performed with direct perturbation and with TSUNAMI-3D-K5. The critical assembly vessel of SHEBA-II consists of a cylindrical tank, which is essentially a 73.7-cm length of 50.8-cm outer-diameter stainless steel pipe. A safety rod thimble with a 6-cm outer diameter passes through the center of the critical assembly vessel. The tank is filled to a critical height of 43.5 cm with a 5% enriched solution of UO₂F₂ and water. Direct perturbation results were obtained by varying the ²³⁵U and ¹H number densities independently and calculating k_{eff} with the perturbed 3-D models using KENO V.a in the CSAS25 SCALE sequence. In the TSUNAMI-3D-K5 model, the fuel was divided into a total of 15 regions. Scoping calculations revealed that no significant changes in the sensitivity results were realized by further dividing the geometry. The forward analysis was performed with 5000 particles per generation and 1000 generations. The sensitivity coefficients were generated using the S_{10} quadrature set, with the flux moments expanded to third order, and the 44-group ENDF/B-V library of SCALE. The TSUNAMI-3D-K5 computed sensitivity of k_{eff} to the total cross section of ²³⁵U is 0.2508 ± 0.0004 , which statistically agrees with the direct perturbation result of 0.2478 ± 0.0084 . For the ¹H total, the TSUNAMI-3D-K5 sensitivity coefficient of 0.2822 ± 0.0087 statistically agrees with the direct perturbation result of 0.2897 ± 0.0078 .

V. SUMMARY AND CONCLUSIONS

Methods for calculating k_{eff} sensitivity coefficients to multigroup cross-section data have been derived for application with Monte Carlo methods. These sensitivity coefficients are calculated with adjoint-based first-order linear perturbation theory. This methodology requires the calculation of the moments of the forward and adjoint neutron fluxes. New methods for the calculation of the flux moments and angular fluxes within Monte Carlo codes via a coordinate transform have been devised.

This new methodology has been implemented into the new TSUNAMI-3D control module within the SCALE code system. The analysis sequences of TSUNAMI-3D use input that is very similar to the CSAS25 SCALE sequence commonly used for criticality safety analysis. The TSUNAMI-3D-K5N analysis sequence performs automated problem-dependent multigroup cross-section processing with BONAMI, NITAWL-III, and MIPLIB. The TSUNAMI-3D-K5 analysis sequence performs automated problem-dependent multigroup cross-section processing and computes the sensitivity of the multigroup data to input quantities through BONAMIST, NITAWLST,

and SENLIB. The forward and adjoint flux solutions necessary for the generation of the sensitivity coefficients are computed using an enhanced version of KENO V.a. The newly created SAMS module uses these flux solutions and the problem-dependent cross-section data to produce sensitivity coefficients. Sensitivity coefficients are automatically produced for every reaction of every nuclide in every region of the system model. With proper specification of the problem geometry, to obtain adequate resolution of the neutron fluxes, TSUNAMI-3D-K5 has been demonstrated to show good agreement with direct perturbation sensitivity coefficients. TSUNAMI-3D produces sensitivities in a number of convenient formats for further analysis either manually or with other automated techniques. Using sensitivity parameters generated from 3-D models with TSUNAMI-3D, the number of critical experiments and applications that can be analyzed with S/U techniques has been greatly increased.

Future work on the methodology employed by TSUNAMI-3D may include development of biasing techniques to aid in the production of the multigroup adjoint flux solutions and methods for geometry division to ensure proper resolution of the fluxes. The techniques implemented into KENO V.a may also be used to develop a sensitivity analysis sequence using the generalized geometry multigroup Monte Carlo code KENO-VI.

ACKNOWLEDGMENTS

The author acknowledges the assistance of L. M. Petrie of the Oak Ridge National Laboratory Nuclear Science and Technology Division for his assistance and advice in the development of the work described in this paper. The author also acknowledges the U.S. Department of Energy (DOE) Environmental Management Science Program, which provided the initial 3 years of project funding, and DOE Nuclear Criticality Safety Program, which, through Environmental Management and Defense Programs, has provided continued funding for this research. The assistance of W. C. Carter in the preparation of this manuscript is greatly appreciated.

Oak Ridge National Laboratory is managed by UT-Battelle, LLC, for the U.S. Department of Energy under contract DE-AC05-00OR22725.

REFERENCES

1. J. H. MARABLE and C. R. WEISBIN, "Theory and Application of Sensitivity and Uncertainty Analysis," ORNL/RSIC-42, Oak Ridge National Laboratory (1979).
2. H. H. HUMMEL and D. OKRENT, *Reactivity Coefficients in Large, Fast Power Reactors*, American Nuclear Society, La Grange Park, Illinois (1979).
3. B. L. BROADHEAD, C. M. HOPPER, and C. V. PARKS, "Sensitivity and Uncertainty Analyses Applied to Criticality

Safety Validation, Volume 2: Illustrative Applications and Initial Guidance," NUREG/CR-6655, Vol. 2 (ORNL/TM-13692/V2), U.S. Nuclear Regulatory Commission, Oak Ridge National Laboratory (1999).

4. B. L. BROADHEAD, B. T. REARDEN, C. M. HOPPER, J. J. WAGSCHAL, and C. V. PARKS, "Sensitivity- and Uncertainty-Based Criticality Safety Validation Techniques," submitted to *Nucl. Sci. Eng.*

5. "SCALE: A Modular Code System for Performing Standardized Computer Analyses for Licensing and Evaluations," NUREG/CR-0200, Rev. 6 (ORNL/NUREG/CSD-2/R6), Vols. I, II, and III, CCC-545, Radiation Safety Information Computational Center at Oak Ridge National Laboratory (2000).

6. R. L. CHILDS, "SEN1: A One Dimensional Cross Section Sensitivity and Uncertainty Module for Criticality Safety Analysis," NUREG/CR-5719 (ORNL/TM-13738), U.S. Nuclear Regulatory Commission, Oak Ridge National Laboratory (1999).

7. "MCNP—A General Monte Carlo N-Particle Transport Code, Version 4B," LA-12625-M, J. F. BRIESMEISTER, Ed., Los Alamos National Laboratory (1997).

8. R. D. O'DELL and R. E. ALCOUFFE, "Transport Calculations for Nuclear Analyses: Theory and Guidelines for Effective Use of Transport Codes," LA-10983-MS, Los Alamos National Laboratory (1987).

9. E. E. LEWIS and W. F. MILLER, Jr., *Computational Methods of Neutron Transport*, American Nuclear Society, La Grange Park, Illinois (1993).

10. L. L. CARTER and E. D. CASHWELL, "Particle-Transport Simulation with the Monte Carlo Method," TID-26607, U.S. Energy Research and Development Administration (1975).

11. C. R. WEISBIN et al., "Application of FORSS Sensitivity and Uncertainty Methodology to Fast Reactor Benchmark Analysis," ORNL/TM-5563, Union Carbide Corporation, Oak Ridge National Laboratory (1976).

12. M. L. WILLIAMS, B. L. BROADHEAD, and C. V. PARKS, "Eigenvalue Sensitivity Theory for Resonance-Shielded Cross Sections," *Nucl. Sci. Eng.*, **138**, 17 (2001).

13. N. M. GREENE, W. E. FORD III, L. M. PETRIE, and J. W. ARWOOD, "AMPX-77: A Modular Code System for Generating Coupled Multigroup Neutron-Gamma Cross-Section Libraries from ENDF/B-IV and/or ENDF/B-V," ORNL/CSD/TM-283, Martin Marietta Energy Systems, Inc., Oak Ridge National Laboratory (1992).

14. R. J. LaBAUVE, "Bare, Highly Enriched Uranium Sphere (GODIVA)," *International Handbook of Evaluated Criticality Safety Benchmark Experiments*, Vol. II, NEA/NSC/DOC(95), Nuclear Energy Agency Nuclear Science Committee of the Organization for Economic Cooperation and Development (2000).

15. R. E. ALCOUFFE, R. S. BAKER, F. W. BRINKLEY, D. R. MARR, R. D. O'DELL, and W. F. WALTERS, "DANTSYS: A Diffusion Accelerated Neutral Particle Transport Code System," LA-12969-M, Los Alamos National Laboratory (1995).

16. J. E. HORWEDEL, "GRESS Version 2.0 User's Manual," ORNL/TM-11951, Martin Marietta Energy Systems, Inc., Oak Ridge National Laboratory (1991).

17. P. R. BEVINGTON, *Data Reduction and Error Analysis for the Physical Sciences*, McGraw-Hill Book Company, New York (1969).

18. W. C. JORDAN, N. F. LANDERS, and L. M. PETRIE, "Validation of KENO V.a Comparison with Critical Experiments," ORNL/CSD/TM-238, Martin Marietta Energy Systems, Inc., Oak Ridge National Laboratory (1986).

19. R. J. LaBAUVE, "Unreflected $\text{UO}_2\text{F}_2 + \text{H}_2\text{O}$ Cylindrical Assembly SHEBA-II," *International Handbook of Evaluated Criticality Safety Benchmark Experiments*, NEA/NSC/DOC(95), Vol. IV, Nuclear Energy Agency Nuclear Science Committee of the Organization for Economic Cooperation and Development (2000).

20. K. B. BUTTERFIELD, "The SHEBA Experiment," *Trans. Am. Nucl. Soc.*, **70**, 199 (1994).